Dynamic Incentive Pricing for Demand Response Programs Based on in-Use Appliances Utilizing Non-Intrusive Load Monitoring

Parsa Eslami[1], Amir Abdollahi[1,*], and Masoud Rashidinejad[1]

[1] *Electrical Engineering Department, Shahid Bahonar University of Kerman, Kerman, Iran*
**Corresponding author: a.abdollahi@uk.ac.ir*

Manuscript received 19 March, 2024; revised 30 May, 2024; accepted 12 June, 2024. Paper no. JEMT-2403-1499.

Demand response programs (DRPs) have gained significant importance in optimizing power systems by reducing peak demand, enhancing grid stability, promoting energy efficiency, and facilitating the integration of renewable energy sources. This paper introduces a novel approach for DRPs by utilizing dynamic incentive pricing strategies with in-use appliances. The proposed approach aims to incentivize consumers to curtail their energy consumption during peak periods, thereby alleviating strain on the grid. In order to address the challenges faced by existing DRPs in accurately monitoring appliance-level energy usage, this paper adopts non-intrusive load monitoring (NILM) as a powerful tool for monitoring and analyzing energy consumption patterns at the appliance level. The implemented DRP in this study is direct load control (DLC), complemented by the sequence to point (seq2point) algorithm for NILM. The proposed approach exhibits several advantages over traditional DRPs. Firstly, it enhances the accuracy of monitoring by utilizing NILM, allowing for appliance-level energy consumption analysis. Secondly, the dynamic incentive pricing strategy creates a financial incentive for consumers to reduce their energy consumption during peak periods, resulting in reduced strain on the grid and overall energy costs. The effectiveness of the proposed approach is evaluated through comprehensive economical and technical analyses. The results demonstrate its superiority compared to traditional DRPs. Notably, the proposed approach achieves a 15.7% reduction in peak demand and a 4% decrease in overall energy consumption. Furthermore, it significantly improves the load factor and peak-to-valley ratio, indicating enhanced grid stability and better utilization of energy resources.

Keywords: *Demand response programs, Dynamic incentive, Non-intrusive load monitoring, In-use appliances, Sequence to point.*

http://dx.doi.org/10.22109/jemt.2024.449080.1499

Nomenclature

Sets

f	f^{th}feature
i	i^{th}hour
j	j^{th}hour
l	l^{th}layer
m	Number of appliances
t	Time

Parameters and Variables

B	Customer bill after demand response
B_0	Customer bill based on initial consumption
b	Bias of features
d	Consumption after demand response
d_0	Initial consumption
$d^{NILM}_{agg,norm\ t:t+W-1}$	Input sliding window
$d^{dataset}_{app}$	Actual consumption of an appliance
d^{NILM}_{app}	An appliance's consumption
$d^{NILM}_{app(k)\ t:t+W-1}$	Output sliding window
$d^{NILM}_{app(k)\ \tau}$	Midpoint of output sliding window
d_{total}	Total consumption after demand response
d^{NILM}_{κ}	Aggregated or extracted power consumption
$d^{NILM}_{\kappa,norm}$	Value calculated by z-score normalization
$\bar{d}^{NILM}_{\kappa}$	Mean value of aggregated or extracted power consumption

E	Price elasticity of demand
$E(i,i)$	Self-elasticity
$E(i,j)$	Cross-elasticity
EC	Energy consumption
EC_{RDC}	Energy consumption reduction
F_P	Sequence to point function
INC	Total paid incentive
inc	Incentive of demand response programs
inc_{app}	An appliance's incentive
inc^{NILM}	Dynamic incentive derived from NILM
L_P	Loss function
LF	Load factor
N	Number of time points
$P2V$	Peak-to-valley
pen	Penalty of demand response programs
$Peak_{RDC}$	Peak reduction
S	Customer benefit after demand response
T	Length of input signal
W	Size of sliding window
$\alpha^{contract}$	Implementation capacity of DRPs
Γ	Activation function
ε	Error of disaggregation
ζ	Decision variable for DLC or NILM parameters
θ	Neural networks parameters
κ	Decision variable for aggregate or appliance consumption
ρ	Spot electricity price
ρ_0	Initial electricity price
σ	Standard deviation
υ	Kernels
ϑ	Size of kernel
ψ	Convolution output

Acronyms

CNN	Convolutional Neural Network
DLC	Direct Load Control
DR	Demand Response
$DRPs$	Demand Response Programs
EP	End of Peak
IBP	Incentive-Based Programs
IRR	Iranian Rial
MAE	Mean Absolute Error
$NILM$	Non-Intrusive Load Monitoring
$seq2point$	Sequence-to-Point
SP	Start of Peak
TBR	Time-Based Rate

1. Introduction

Energy consumption reduction is of paramount importance and cannot be overlooked in the present times. With the rapid industrialization of society, the demand for electricity is steadily increasing, while the global population continues to grow. This escalating demand puts significant strain on the Earth's limited energy resources. The Industrial Revolution, which began in the 18th century, marked the onset of an era characterized by extensive energy consumption, predominantly reliant on fossil fuels like coal, oil, and natural gas. However, the utilization of these finite fuel sources comes at a cost, contributing to climate change, a global crisis that poses a substantial threat to both the environment and human livelihoods. This paper explores the significance of reducing energy usage and discusses the consolidation of demand response programs (DRPs) and non-intrusive load monitoring (NILM). It should be acknowledged that the mentioned aspects will be feasible and executable when integrated within smart grid framework.

Demand response (DR) is a widely used approach for conserving energy and improving efficiency. It involves adjusting energy consumption by reducing, eliminating, or changing loads to balance power supply and demand. DR plays a critical role in enhancing the reliability of modern electrical grids [1]. In December 2022, the Federal Energy Regulatory Commission (FERC) issued a report detailing the outcomes of demand response initiatives in the utilities and electricity markets in the United States [2]. The FERC report classified demand response programs into two primary categories: time-based rate (TBR) programs and incentive-based programs (IBPs). TBR programs, such as time of use (TOU), real-time pricing (RTP), and critical peak pricing (CPP), involve variations in electricity prices during different time periods based on the cost of electricity supply. In these programs, there is no specific incentive or penalty provided to encourage customer response [3]. IBPs can be categorized into three primary subgroups: voluntary, mandatory, and market clearing programs. Voluntary programs, such as direct load control (DLC) and emergency demand response program (EDRP), allow customers to participate on a voluntary basis, and they are not penalized if they choose not to curtail their energy consumption. On the other hand, mandatory programs like interruptible/ curtailable (I/C) and capacity market program (CAP) require enrolled customers to curtail their energy usage when directed. Failure to comply with the curtailment instructions may result in penalties or consequences for the customers. Market clearing programs, such as demand bidding (DB) and ancillary services (A/S), operate by encouraging large customers to offer or provide load reductions at a price determined by their willingness to be curtailed. These programs give customers the opportunity to specify the amount of load they are willing to curtail at the posted prices [3]. Numerous studies have explored DRPs in recent years. An economic model for I/C and CAP programs, leveraging price elasticity of demand and customer benefit function is introduced in [4]. The simulation study using real-world data demonstrates the influence of these programs on load characteristics, customer benefits, and energy consumption reduction. The findings provide valuable insights for ISOs and policymakers in identifying effective demand response strategies and prioritizing scenarios. Reference [5] presents a new approach to DRPs that considers the economic factors influencing customer behavior. It builds a nonlinear model based on two key aspects: price elasticity of demand and customer benefit function. The model analyzes how different factors like incentives, penalties, and implementation potential impact the effectiveness of DRPs. It also assesses the reliability of these programs under varying conditions. The results demonstrate that the nonlinear model provides the most conservative estimates, while linear models tend to be less conservative. The optimal operation of power systems in the presence of wind turbines, hydrogen storage systems, and DRPs, considering uncertainties is addressed in [6]. In order to ensure robust operation under the worst-case scenario, a new approach called stochastic p-robust optimization method is proposed. This method combines

stochastic programming and robust optimization techniques to minimize the worst-case cost or regret level. The authors in [7] proposed a novel pricing method for regulating time-based rate demand response called the close-loop reverse Stackelberg game-based approach. The proposed method utilizes a hierarchical game structure, where the lower-level consists of heterogeneous demand-side resources engaging in noncooperative competition during demand response participation. On the other hand, the upper level is responsible for determining the pricing policy. A novel hybrid DR mechanism that considers three key participants: the power grid operator (PGO), retailers, and end users is introduced in [8]. Unlike traditional approaches based on fixed pricing or incentives, this hybrid mechanism combines real-time pricing and real-time incentives to implement DRPs coordinated by the PGO. Essentially, the PGO provides incentives to retailers, who, in turn, determine optimal real-time prices for end users every 5 minutes. By integrating both pricing and incentives, this hybrid DR mechanism effectively motivates retailers to participate by offering them monetary incentives from the PGO to encourage load shifting. NILM, as a technology, complements demand response programs by providing accurate insights into the energy consumption of specific appliances without the need for in-home measurement devices. This technology enables consumers to identify high-energy-consuming devices, discover usage patterns, and make informed decisions about energy conservation. Following this introduction, detailed explanations about NILM will be provided.

In recent years, advancements in advanced metering technology have facilitated efficient management, monitoring, and regulation of the distribution grid. This progress has led to improved energy utilization and significant energy savings. One enabling technology is NILM, which offers a service that estimates the energy usage of individual appliances within a building without the need for any physical modifications or interventions. By leveraging NILM, energy consumption can be effectively monitored and regulated, contributing to better energy management and overall energy conservation. In the early stages of NILM research, Hidden Markov models were commonly used for probabilistic modeling of time series data [9]. Optimization methods offered an alternative approach, focusing on finding the optimal combination of individual appliances within the aggregated energy signal [10]. Shallow learning techniques, encompassing conventional classification and regression algorithms such as support vector machines [11], naive bayes classifiers [12], k-nearest neighbors [13], tree-based implementations [14], and XGBoost [15], were also employed in NILM studies. Deep learning models, including feed-forward neural networks [16], convolutional neural networks [17], and recurrent neural networks [18], have gained popularity in recent years due to their exceptional performance in various tasks. Moreover, cutting-edge deep learning techniques such as deep generative models [19], transfer learning [20], and federated learning [21] have been applied in the field of NILM to further advance its capabilities.

This paper presents the development of an economic model for DRPs that incorporates the concept of “price elasticity of demand”. The model focuses on incentive responsive loads and their ability to adjust their electricity consumption based on changes in incentives. This paper primarily examines voluntary incentive-based programs, namely DLC and EDRP. These programs operate under the premise that the independent system operator (ISO) provides incentives to customers for reducing their load, but does not impose penalties for non-compliance. A novel approach is introduced for these programs, which involves the implementation of a dynamic incentive pricing strategy based on NILM. The proposed framework focuses on integrating in-use appliance data using NILM. It utilizes the sequence-to-point (seq2point) methodology to extract appliance consumption information from aggregated load data collected by smart meters. The paper will provide a detailed explanation of this methodology, offering a comprehensive understanding of its implementation. Additionally, the framework incorporates dynamic incentive pricing strategies that aim to motivate customers to reduce their energy consumption during demand response events. In summary, this paper aims to present a new model for demand response programs using non-intrusive load monitoring and it introduces a dynamic incentive function that is dependent on appliances consumption ($inc^{NILM}(d_{app}^{NILM})$) during peak hours. Eventually, demand response planning will be conducted based on this new incentive, and it will be analyzed both technically and economically.

The rest of this paper is organized as follows. Section 2 proposes the structure of the paper. Afterwards, section 3 introduces the carried-out mathematical model and simulations. Furthermore, the investigated case study and the results are discussed in detail in section 4. Finally, conclusions are presented in section 5.

2. Proposed $inc^{NILM}(d_{app}^{NILM})$ Structure

In this section, the proposed framework for calculating dynamic incentive pricing ($inc^{NILM}(d_{app}^{NILM})$) and modeling NILM-based DR is explained. As depicted in Fig. 1, the modeling process of this paper consists of three stages. In the first stage, data is collected and then organized, and the inputs are configured using sliding window method. Finally, in this stage, the data is normalized.

In the second stage, which involves the implementation of NILM, the corresponding neural network is designed, trained, and tested. Once satisfactory results are obtained from the testing phase, the final NILM results are calculated.

In the third stage, the incentive for each hour is calculated based on the results obtained in the second stage, which is the most important step. Subsequently, the direct load control program is executed based

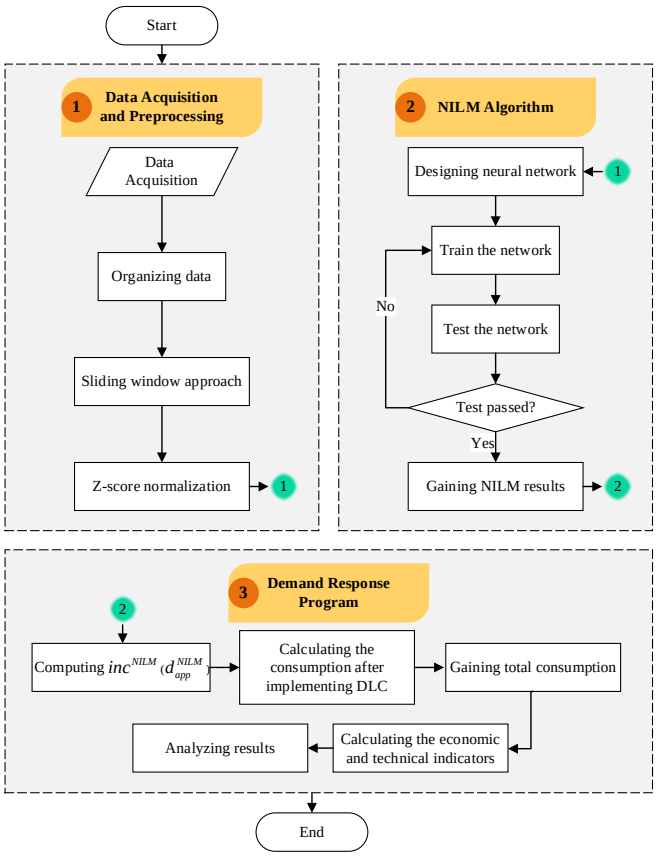

Fig. 1. The proposed structure for modeling NILM-based DR using $inc^{NILM}(d_{app}^{NILM})$

on the calculated incentives, and the overall energy consumption is determined. Furthermore, the technical and economic indicators of the demand response program are calculated, and the results are analyzed.

3. Mathematical Formulation

In this paper, the effect of in-use appliances on dynamic incentive pricing based on non-intrusive load monitoring for demand response applications has been employed. In this section, the mathematical formulation of the introduced structure is presented.

3.1. Data Acquisition and Preprocessing

The first step of simulating the structure is collecting aggregated consumption data and the consumption of each appliance from some households. The selected household appliances include evaporative cooler, air conditioner, lighting, and other devices.

Data obtained from sensors or smart meters often need to be improved. In addition, for processing by predictive algorithms, a necessary step is data preprocessing, which involves converting raw data into a suitable format for training and evaluation. The sliding window approach is a widely used technique for converting signal data into the input format required by neural networks. This method involves dividing historical data into smaller sequences with a fixed length, which overlap with each other [22].

Feature scaling or data normalization is an important step in neural network training. This helps avoid issues like vanishing gradients or explosions and speeds up the learning process [23]. In this study, z-score normalization technique is used for feature scaling. It involves calculating the mean and standard deviation of the main and sub-metered from the entire training set [24]. This technique is represented by the following equation:

$$d_{\kappa,norm}^{NILM} = \frac{d_{\kappa}^{NILM}(t) - \bar{d}_{\kappa}^{NILM}}{\sigma}$$
$$\forall \kappa = \begin{cases} agg \\ app \end{cases} \quad (1)$$

where $d_{\kappa}^{NILM}(t)$ represents the aggregate or extracted power consumption at time t, $\bar{d}_{\kappa}^{NILM}$ denotes the mean value of a main or appliance reading, and σ represents the standard deviation.

3.2 Sequence-to-Point Learning

Seq2point learning has surfaced as a highly promising method with significant potential for utilization in NILM systems. [20]. In the past, NILM methods predominantly relied on seq2seq models, which aimed to match aggregate energy data sequences to individual appliance activation sequences. Nevertheless, these seq2seq models were computationally demanding and demanded extensive training data. Seq2point learning, on the other hand, emerges as a more efficient and effective alternative for NILM, offering improved computational efficiency and data requirements. It simplifies the learning task by directly predicting the midpoint element of the target appliance's window from the mains window input. Seq2point models, in contrast to their seq2seq counterparts, concentrate on directly predicting the specific points of appliance activations from the aggregate energy data. This streamlined approach simplifies the learning process, decreases computational complexity, and potentially reduces the amount of training data needed [25]. In order to provide more specificity, in seq2point learning for NILM, the neural network takes a specific time window of aggregate energy data (referred to as the mains window) as input. The network then predicts the midpoint element (referred to as the output) of the corresponding time window representing the energy consumption of a specific appliance of interest. The mains window, which shown by $d^{NILM}_{agg,norm\ t:t+W-1}$, produces the midpoint element $d^{NILM}_{app(k)\ \tau}$. The τ is represents as:

$$\tau = t + \left\lfloor \frac{W}{2} \right\rfloor \quad (2)$$

where W is size of the sliding window. According to this statement, it is implied that the relationship between the midpoint element and the main window is expected to be non-linear. This assumption arises from the anticipation that the midpoint element's state in a particular device will be influenced by the data from the main power source both preceding and following that midpoint. The seq2point models establish a neural network labeled as F_p, which takes the sliding windows $d^{NILM}_{agg,norm\ t:t+W-1}$ from the input and maps them to the midpoint $d^{NILM}_{app(k)\ \tau}$ of the corresponding windows $d^{NILM}_{app(k)\ t:t+W-1}$ of the output. The model is formulated such that the midpoint element is equal to a function of the sliding windows from the input, with an added error term ε, which is shown in (3).

$$d^{NILM}_{app(k)\ \tau} = F_p(d^{NILM}_{agg,norm\ t:t+W-1}) + \varepsilon \quad (3)$$

Since this model uses one-dimensional convolutional layer and the input is in vector form, considering $\upsilon(t)$ as a kernel with size ϑ, the convolution output $\psi(t)$ can be computed as follows [26].

$$\psi(t) = d^{NILM}_{agg,norm}(t) * \upsilon(t) = \sum_{c=1}^{\vartheta} \upsilon(c) \times d^{NILM}_{agg,norm}(t-c)$$
$$\forall\ t = [1, N] \quad (4)$$

where "$*$" represents the convolution operation. In a broader sense, the convolved features obtained at the output of the l^{th} layer can be expressed as [26]:

$$\psi_f^l = \Gamma\left(b_f^l + \sum_g \psi_g^{l-1} \times \upsilon_{fg}^l\right) \quad (5)$$

In this regard, ψ_f^l denotes the f^{th} feature in the l^{th} layer, ψ_g^{l-1} indicates the g^{th} features in the $(l-1)^{th}$ layer, υ_{fg}^l symbolizes the kernel linked from the f^{th} to the g^{th} features, b_f^l conveys the bias for these features, and Γ signifies the activation function.

The activation function implemented in this paper is rectified linear unit (ReLU), which is formulated as follows [27].

$$\Gamma(t) = \mathrm{Max}(0, t) \quad (6)$$

The loss function utilized to evaluate the error or loss during the training process is [20]:

$$L_p = \sum_{t=1}^{T-W+1} \log p\left(d^{NILM}_{app(k)\ \tau} \mid d^{NILM}_{agg,norm\ t:t+W-1}, \theta\right) \quad (7)$$

where θ is used to represent the parameters of the neural network being trained and T is length of input signal. In the subsequent sections of this paper, the midpoint element which is used as the output of the neural network is represented as $d^{NILM}_{app(k)}$ instead of $d^{NILM}_{app(k)\ \tau}$ for simplicity.

The Adam optimizer algorithm [28] is employed to update the model parameters during training. This method calculates individual adaptive learning rates for various parameters using estimates of the gradients' first and second moments. Adam optimizer has four main parameters. The first parameter is learning rate, which controls the step size during model updates. The second and third parameters are exponential decay rate for the first and second moments estimates, respectively. These parameters are called Beta1 and Beta2. The last parameter is Epsilon, that is a small constant added for numerical stability.

This paper utilizes the mean absolute error (MAE) metric to evaluate the performance of the NILM algorithm. MAE is the average

difference between the predicted value ($d_{app(k)}^{NILM}$) and the actual value ($d_{app(k)}^{dataset}$) for each time point measurement. It measures the average magnitude of the errors without considering their direction, providing a straightforward assessment of the prediction accuracy.

$$MAE = \frac{1}{N}\sum_{t=1}^{N}\left|d_{app(k),\,t}^{NILM} - d_{app(k),\,t}^{dataset}\right| \quad (8)$$

In this context, N represents the number of time points, indicating the total number of measurements used to calculate MAE.

3.3 Direct Load Control

DLC, as a voluntary incentive-based demand response program, implies that customers will not face negative consequences or penalties if they choose not to reduce their energy consumption. [29]. The general equation for DRPs can be expressed as follows [30]:

$$d(i) = d_0(i) \times \left\{1 + E(i,i) \times \frac{\rho(i)-\rho_0(i)+inc(i)+pen(i)}{\rho_0(i)} + \sum_{\substack{j=1\\ j\neq i}}^{24} E(i,j) \times \frac{\rho(j)-\rho_0(j)+inc(j)+pen(j)}{\rho_0(j)}\right\}$$
$$\forall i = 1,2,3,\ldots,24 \quad (9)$$

where $d_0(i)$ is initial consumption in i^{th} hour, $d(i)$ is consumption after utilizing DR, $E$is price elasticity of demand which, $E(i,i)$ and $E(i,j)$ are self-elasticity and cross-elasticity respectively. $\rho$and $\rho_0$is spot and initial electricity prices individually. Finally, inc is incentive and $pen$is penalty of DRPs.

An important contribution of this paper is the consideration that the incentive in the discussed article is not constant but varies on an hourly basis, depending on household appliance consumption. The calculation of this value is determined by the following equation:

$$inc^{NILM-based\ DLC}(i) = \frac{\sum_{k=1}^{m} d_{app(k)}^{NILM}(i) \times inc_{app(k)}}{\sum_{k=1}^{m} d_{app(k)}^{NILM}(i)} \quad (10)$$

where m is the number of appliances, $d_{app(k)}^{NILM}(i)$ is consumption of k^{th} appliance in i^{th} hour, and $inc_{app(k)}$ is the incentive of k^{th} appliance. Given this equation and considering that the DLC program is the focus of this paper, equation (6) can be rewritten as follows:

$$d^{\zeta}(i) = d_0(i) \times \left\{1 + E(i,i) \times \frac{inc^{\zeta}(i)}{\rho_0(i)} + \sum_{\substack{j=SP\\ j\neq i}}^{EP} E(i,j) \times \frac{inc^{\zeta}(j)}{\rho_0(j)}\right\}$$
$$\forall i \in [SP, EP]$$
$$\forall \zeta = \begin{cases} DLC \\ NILM - based\ DLC \end{cases} \quad (11)$$

where SP is start of peak time and EP is end of it. The value of i also changes during this interval. Since both the regular demand response program and the non-intrusive load monitoring-based demand response program are utilized in this paper, the parameter ζ is used to differentiate and separate them in the equations.

The implementation capacity of DRPs is considered as $\alpha^{contract}$. This means that the number of contracts signed with participating customers in these programs is equivalent to $\alpha^{contract}$ percent of the total energy load. Considering this matter, the overall consumption after implementing the DLC program, based on the results of non-intrusive load monitoring represented as d_{total}^{ζ} , will be as follows.

$$d_{total}^{\zeta}(i) = \alpha^{contract} \times d^{\zeta}(i) + (1 - \alpha^{contract}) \times d_0(i)$$
$$\forall i = 1,2,3,\ldots,24$$
$$\forall \zeta = \begin{cases} DLC \\ NILM - based\ DLC \end{cases} \quad (12)$$

Customers modify their energy demand from the initial value, $d_0(i)$, to $d^{\zeta}(i)$, influenced by the incentive outlined in the contractual agreement. The total incentive provided to customers for their participation in demand response programs can be computed by multiplying the payment of $inc^{\zeta}(i)$ per kilowatt-hour (kWh) of load reduction during the i^{th} hour.

$$INC^{\zeta} = \sum_{i=SP}^{EP} inc^{\zeta}(i) \times [d_0(i) - d^{\zeta}(i)] \times \alpha^{contract}$$
$$\forall \zeta = \begin{cases} DLC \\ NILM - based\ DLC \end{cases} \quad (13)$$

Let B^{ζ} represent the customer's bill after engaging in demand response, and B_0 denote the customer's bill without utilizing demand response. In such a scenario, the customer's benefit (S^{ζ}) can be determined using the following calculation:

$$S^{\zeta} = B_0 - B^{\zeta} + INC^{\zeta}$$
$$\forall \zeta = \begin{cases} DLC \\ NILM - based\ DLC \end{cases} \quad (14)$$

It is apparent that the peak value corresponds to the maximum value of d_{total}^{ζ}. Therefore, the percentage reduction of the peak can be calculated using the following equation:

$$Peak_{RDC}^{\zeta} = \frac{peak(d_0) - peak^{\zeta}(d_{total}^{\zeta})}{peak(d_0)} \times 100$$
$$\forall \zeta = \begin{cases} DLC \\ NILM - based\ DLC \end{cases} \quad (15)$$

It is understood that the energy consumption is the sum of power consumptions over a 24-hour period shown in (16).

$$EC^{\zeta} = \sum_{i=1}^{24} d_{total}^{\zeta}(i)$$
$$\forall \zeta = \begin{cases} DLC \\ NILM - based\ DLC \end{cases} \quad (16)$$

The percentage reduction in energy consumption can be calculated using equation (17):

$$EC_{RDC}^{\zeta} = \frac{EC(d_0) - EC^{\zeta}(d_{total}^{\zeta})}{EC(d_0)} \times 100$$
$$\forall \zeta = \begin{cases} DLC \\ NILM - based\ DLC \end{cases} \quad (17)$$

The load factor serves as an indicator of the efficiency and utilization of an electrical system, representing the ratio of the average power demand to the maximum power demand within a specified timeframe. It quantifies how effectively the system's capacity is being utilized and is computed by dividing the total energy consumed by the product of the maximum demand and the time period, as described in equation (18). A higher load factor indicates a more efficient utilization of the system's capacity, leading to reduced energy waste and enhanced operational efficiency.

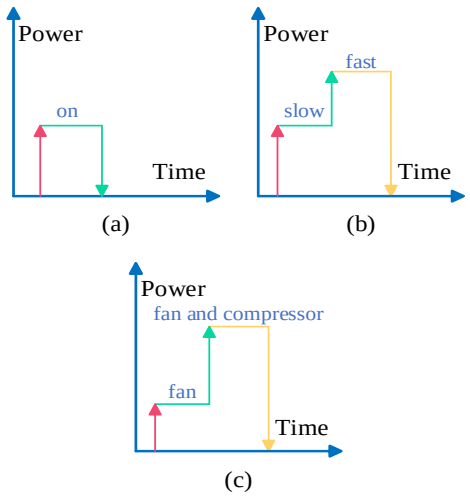

Fig. 2. Load signatures of appliances: (a) Lighting; (b) Evaporative cooler; (c) Air conditioner

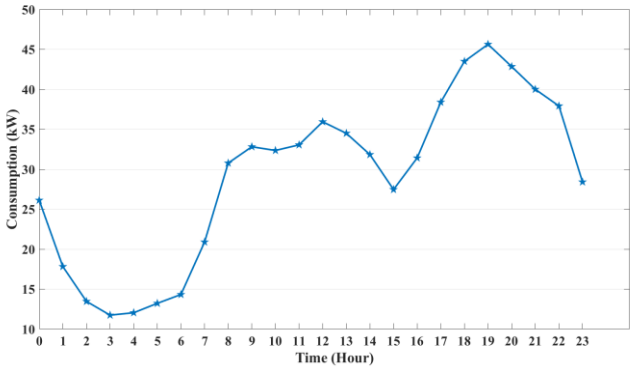

Fig. 3. Initial total consumption of households

$$LF^{\zeta} = \frac{EC^{\zeta}}{peak^{\zeta}(d^{\zeta}_{total})\times 24} \times 100$$

$$\forall\zeta = \begin{cases} DLC \\ NILM - based\ DLC \end{cases} \quad (18)$$

Peak-to-valley refers to the duration between the highest energy consumption peak and the lowest energy consumption valley observed during a specified timeframe. This measure enables the evaluation of variability and fluctuations in energy demand, offering insights into the system's load profile and the potential for load shifting strategies. As this paper does not explore shiftable demand response, the timing of peak and valley occurrences remains unchanged. Consequently, the paper focuses solely on investigating the magnitudes of these peaks and valleys.

$$P2V^{\zeta} = Max(d^{\zeta}_{total}) - Min(d^{\zeta}_{total})$$

$$\forall\zeta = \begin{cases} DLC \\ NILM - based\ DLC \end{cases} \quad (19)$$

4. Case Study and Results

This section focuses on the examination of the numerical results obtained from the model presented in previous section. The simulations were conducted using MATLAB software version R2021b and Python version 3.9.10.

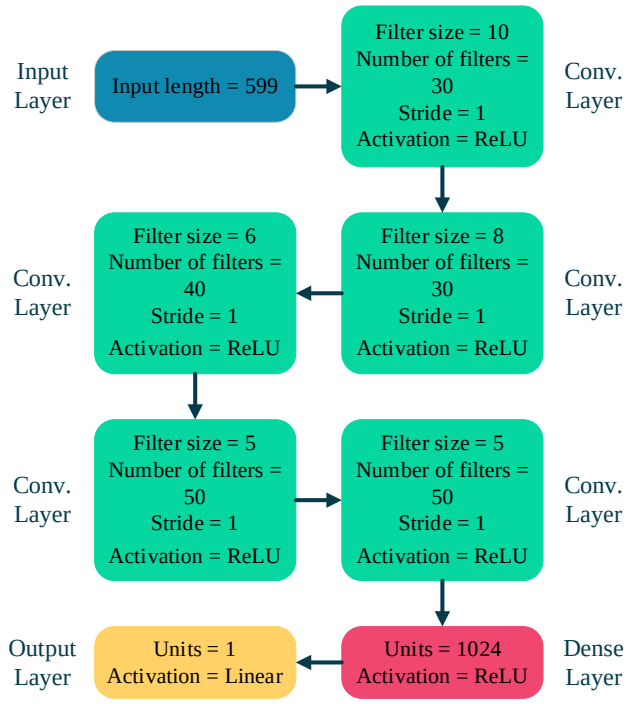

Fig. 4. Seq2point network architecture

At the beginning of this section, the introduction of the system under study in this paper is provided. In order to evaluate the practical feasibility of the proposed model in real-world scenarios, energy consumption data has been collected from thirty households. From these households, energy consumption data of various home appliances from twenty households were utilized for training and testing the seq2point neural network algorithm. However, for the remaining ten households, only aggregated data from smart meters is available. The appliances used in this paper are: "evaporative cooler", "air conditioner", "lighting", and other devices. The load signatures of these appliances are on/off for lighting and finite state machine for evaporative cooler and air conditioner. As the name suggests, the first type has only two states: on and off. However, the devices related to the second type have multiple operational modes. The operational modes of evaporative cooler are low or high fan-speed. For the air conditioner the operational modes are compressor being on or off and fan being on or off. Fig. 2 demonstrates the load signatures of these appliances. In Fig. 2 (a), on and off states of lighting can be observed. Fig. 2 (b) illustrates the states of evaporative cooler's fan, including off, slow, and fast. Fig. 2 (c) represents the states of the air conditioner's fan and compressor, including off for both, only fan is on, and finally, both the fan and compressor are on simultaneously. Furthermore, this paper does not impose any limitations on the usage of these appliances by consumers.

The total consumption of all households is shown in Fig. 3. As depicted in this figure, the peak hours, which are under investigation in this study, fall between hours 17 and 22.

The seq2point network architecture used in this research is depicted in Fig. 4. As evident from the figure, the network begins with an input layer of size 599, which corresponds to the length of the sliding window. Following the input layer, there are five convolutional networks, with the size and number of filters specified in the figure. The stride size for all these layers is one, and the activation function used is ReLU. After the convolutional layers, there is a fully connected (dense) layer where all units are connected to each other. Finally, there is an output layer with a single unit and a linear activation function.

The parameters' values of the Adam optimizer are shown in Table 1 [20].

Table 1. Adam optimizer parameters' values

Parameters	*Learning rate*	*Beta1*	*Beta2*	*Epsilon*
Values	0.001	0.9	0.999	10-8

This paper considers three scenarios for implementing demand response programs. In the first scenario, no demand response program is executed. In the second scenario, a direct load control demand response program is implemented. In the third scenario, the demand response program is based on the results of non-intrusive load monitoring. The electricity price is constant at 4356 Rials per kW for all hours. In the second scenario, the incentive value for all appliances during peak hours is set at 2489 Rials per kW. The incentives considered for the third scenario are listed in Table 2. Furthermore, the implementation capacity of demand response programs ($\alpha^{contract}$) in the second and third scenarios is considered to be fifty percent.

Table 2. Incentive of appliances

Appliance	*Evaporative cooler*	*Air conditioner*	*Lighting*	*Other devices*
Incentive (IRR/kW)	2667	3556	889	2844

Now that the introduction to the system under study in this paper has been presented, the continuation of this section will present and discuss the results of the analysis.

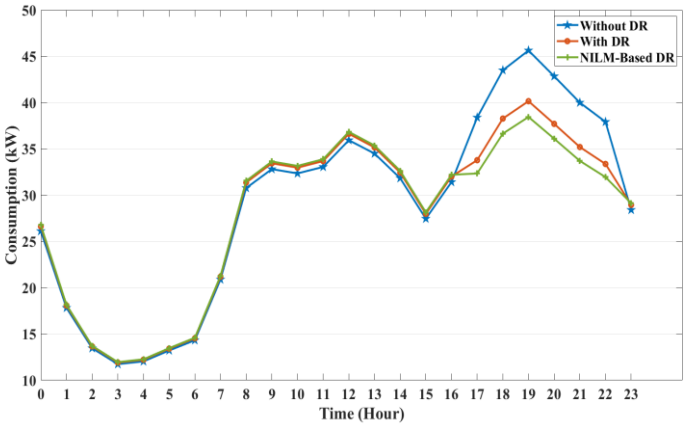

Fig. 6. Total consumption of three scenarios

The performance of the seq2point algorithm is first evaluated based on the MAE metric, as explained earlier, to assess the effectiveness of this NILM approach. The obtained results are presented in Table 3.

Table 3. Seq2point performance evaluation using MAE for each appliance

Appliance	*Evaporative cooler*	*Air conditioner*	*Lighting*
MAE (%)	4.39	2.31	5.52

As evident from the above table, the seq2point algorithm demonstrates satisfactory performance overall during the training and testing phases. It exhibits the highest efficiency for the air conditioner appliance and the lowest efficiency for the lighting. The overall value of this metric, obtained by averaging these values, is denoted as 4.07 percent.

Fig. **5** presents the percentage utilization of various appliances during summer peak hours, as determined using non-intrusive load monitoring techniques. As shown in the figure, the highest energy consumption in the early hours is primarily associated with cooling appliances, which gradually decreases over time. Conversely, the energy consumption of lighting and other devices exhibits an upward trend. On average, during these hours, the percentage of energy consumption for evaporative coolers, air conditioners, lighting, and other appliances is 22%, 29%, 16%, and 33% respectively.

Fig. **6** provided demonstrates the overall energy consumption in three scenarios: without DR, with DR, and NILM-based DR. In the NILM-based DR scenario, the demand response program is based on the results obtained from non-intrusive load monitoring. As depicted in the figure, the implementation of any form of demand response leads to a reduction in peak energy consumption. However, utilizing NILM-based demand response results in a further decrease in electricity usage, contributing to an improved consumption pattern. Numerically, the figure shows that the plain demand response program achieves a 12% reduction in peak consumption, while the NILM-based demand response achieves more than a 15.5% reduction in peak demand. Further in this section, a discussion will be conducted to assess the economic and technical impacts of these three scenarios.

Table 4 presents the economic results, showcasing the outcomes associated with each scenario. It is evident that the implementation of demand response results in a decrease in customer payments. As indicated in the table, the plain demand response program results in an approximate 3.11 percent reduction in the customer's bill. The reduction in the customer's bill becomes even more significant when the NILM-based demand response program is implemented i.e., 4.086%. Additionally, customers receive incentives as a result of their reduced energy consumption. The total incentives received by consumers are 52000 and 89300 Rials, respectively, in accordance with the aforementioned DRPs. These two reasons contribute to the substantial benefit experienced by the customers. Considering the inclusion of 30 households in this study, the calculated benefit per household from implementing DR and NILM-based DR is 4880 and 7110 Rials per house, respectively. Based on these findings, it can be concluded that on a larger scale, particularly with a greater number of households, the last scenario (NILM-based demand response) provides significant cost reduction benefits to customers.

Table 4. Economical results for implementation different DRPs

Scenarios	*Customer bill (Million IRR)*	*Paid incentive (Million IRR)*	*Customer benefit (Million IRR)*
Without DR	3.0337	0	0
With DR	2.9393	0.0520	0.1464
NILM-Based DR	2.9098	0.0893	0.2133

Table **5** presents the technical outcomes, summarizing the results obtained regarding the technical aspects. It is evident that NILM-based demand response performs superiorly in reducing peak demand and overall energy consumption. Furthermore, NILM-based demand response results in a greater improvement in the load factor and the peak-to-valley ratio. Likewise, peak demand and energy consumption have been reduced 16% and 4%, respectively. Considering the calculated percentage reductions in peak demand and energy consumption, it can be expected that even greater reductions in these parameters would occur on a larger scale.

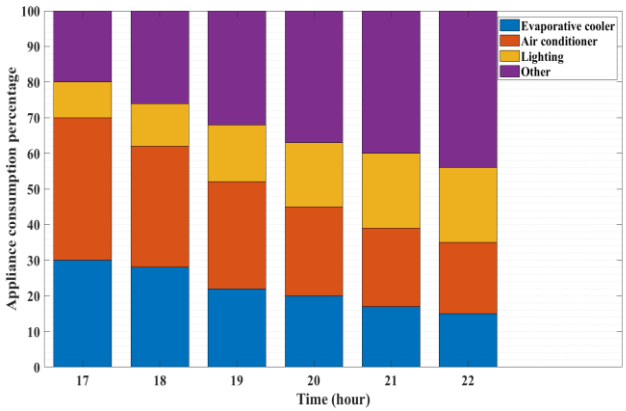

Fig. 5. Appliances consumption percentage in peak hours

Table 5. Technical results for implementation different DRPs

Scenarios	*Peak (kW)*	*Peak reduction (%)*	*Energy consumption (kWh)*	*Consumption reduction (%)*	*Load factor (%)*	*Peak to valley (kW)*
Without DR	45.6330	0	696.4480	0	63.5914	33.8910
With DR	40.1570	12	674.7620	3.1138	70.0128	28.2460
NILM-Based DR	38.4501	15.7406	668.0021	4.0844	72.3884	26.4863

5. Conclusion

This paper introduced a dynamic incentive pricing approach for demand response programs (DRPs), specifically targeting in-use appliances. Extensive research and analysis revealed the limitations of existing DRPs, particularly in accurately monitoring appliance-level energy usage. In order to address these limitations, the paper proposed the utilization of non-intrusive load monitoring (NILM) as a robust tool for monitoring and analyzing energy consumption patterns at the appliance level. By leveraging NILM, the implementation of DRPs becomes more precise and effective. The findings highlighted that the proposed NILM-based DR approach outperforms traditional DRPs in terms of reducing peak demand, energy consumption, and improving the load factor and peak-to-valley ratio. Moreover, customers benefit from reduced energy costs and incentives provided for their lower consumption. It is worth noting that these results were obtained from a study involving 30 households, and it is anticipated that even greater benefits and reductions could be achieved on a larger scale. Overall, the integration of NILM into DRPs has the potential to revolutionize the energy management landscape by enabling more accurate monitoring and efficient utilization of energy resources at the appliance level.

References

[1] S. Poorvaezi-Roukerd, A. Abdollahi, and W. Peng, "Flexibility-constraint integrated resource planning framework considering demand and supply side uncertainties with high dimensional dependencies," *International Journal of Electrical Power and Energy Systems*, vol. 133, 2021, doi: 10.1016/j.ijepes.2021.107223.

[2] "2022 Assessment of Demand Response and Advanced Metering | Federal Energy Regulatory Commission." Accessed: Mar. 13, 2024. [Online]. Available: https://www.ferc.gov/media/2022-assessment-demand-response-and-advanced-metering

[3] C. Ibrahim, I. Mougharbel, H. Y. Kanaan, N. A. Daher, S. Georges, and M. Saad, "A review on the deployment of demand response programs with multiple aspects coexistence over smart grid platform," *Renewable and Sustainable Energy Reviews*, vol. 162. 2022. doi: 10.1016/j.rser.2022.112446.

[4] H. A. Aalami, M. P. Moghaddam, and G. R. Yousefi, "Demand response modeling considering Interruptible/Curtailable loads and capacity market programs," *Appl Energy*, vol. 87, no. 1, 2010, doi: 10.1016/j.apenergy.2009.05.041.

[5] H. A. Aalami, H. Pashaei-Didani, and S. Nojavan, "Deriving nonlinear models for incentive-based demand response programs," *International Journal of Electrical Power and Energy Systems*, vol. 106, 2019, doi: 10.1016/j.ijepes.2018.10.003.

[6] T. Cai, M. Dong, H. Liu, and S. Nojavan, "Integration of hydrogen storage system and wind generation in power systems under demand response program: A novel p-robust stochastic programming," *Int J Hydrogen Energy*, vol. 47, no. 1, 2022, doi: 10.1016/j.ijhydene.2021.10.027.

[7] X. Sun, H. Xie, Y. Xiao, and Z. Bie, "Incentive Compatible Pricing for Enhancing the Controllability of Price-Based Demand Response," *IEEE Trans Smart Grid*, vol. 15, no. 1, 2024, doi: 10.1109/TSG.2023.3279415.

[8] B. Xu, J. Wang, M. Guo, J. Lu, G. Li, and L. Han, "A hybrid demand response mechanism based on real-time incentive and real-time pricing," *Energy*, vol. 231, 2021, doi: 10.1016/j.energy.2021.120940.

[9] M. A. Mengistu, A. A. Girmay, C. Camarda, A. Acquaviva, and E. Patti, "A Cloud-Based On-Line Disaggregation Algorithm for Home Appliance Loads," *IEEE Trans Smart Grid*, vol. 10, no. 3, 2019, doi: 10.1109/TSG.2018.2826844.

[10] K. He, L. Stankovic, J. Liao, and V. Stankovic, "Non-Intrusive Load Disaggregation Using Graph Signal Processing," *IEEE Trans Smart Grid*, vol. 9, no. 3, 2018, doi: 10.1109/TSG.2016.2598872.

[11] F. Gong, N. Han, Y. Zhou, S. Chen, D. Li, and S. Tian, "A SVM Optimized by Particle Swarm Optimization Approach to Load Disaggregation in Non-Intrusive Load Monitoring in Smart Homes," in *2019 3rd IEEE Conference on Energy Internet and Energy System Integration: Ubiquitous Energy Network Connecting Everything, EI2 2019*, 2019. doi: 10.1109/EI247390.2019.9062124.

[12] C. C. Yang, C. S. Soh, and V. V. Yap, "A non-intrusive appliance load monitoring for efficient energy consumption based on Naive Bayes classifier," *Sustainable Computing: Informatics and Systems*, vol. 14, 2017, doi: 10.1016/j.suscom.2017.03.001.

[13] F. Hidiyanto and A. Halim, "KNN Methods with Varied K, Distance and Training Data to Disaggregate NILM with Similar Load Characteristic," in *ACM International Conference Proceeding Series*, 2020. doi: 10.1145/3400934.3400953.

[14] Z. Xiao, W. Gang, J. Yuan, Y. Zhang, and C. Fan, "Cooling load disaggregation using a NILM method based on random forest for smart buildings," *Sustain Cities Soc*, vol. 74, 2021, doi: 10.1016/j.scs.2021.103202.

[15] Z. Chen, J. Chen, X. Xu, S. Peng, J. Xiao, and H. Qiao, "Non-intrusive load monitoring based on feature extraction of change-point and xgboost classifier," in *2020 IEEE 4th Conference on Energy Internet and Energy System Integration: Connecting the Grids Towards a Low-Carbon High-Efficiency Energy System, EI2 2020*, 2020. doi: 10.1109/EI250167.2020.9347014.

[16] R. C. Lekshmi *et al.*, "Non-intrusive Load Monitoring with ANN-Based Active Power Disaggregation of Electrical Appliances," 2021. doi: 10.1007/978-981-33-6691-6_41.

[17] F. Ciancetta, G. Bucci, E. Fiorucci, S. Mari, and A. Fioravanti, "A New Convolutional Neural Network-Based System for NILM Applications," *IEEE Trans Instrum Meas*, vol. 70, 2021, doi: 10.1109/TIM.2020.3035193.

[18] M. Kaselimi, N. Doulamis, A. Voulodimos, E. Protopapadakis, and A. Doulamis, "Context Aware Energy Disaggregation Using Adaptive Bidirectional LSTM Models," *IEEE Trans Smart Grid*, vol. 11, no. 4, 2020, doi: 10.1109/TSG.2020.2974347.

[19] A. Langevin, M. Cheriet, and G. Gagnon, "Efficient deep generative model for short-term household load forecasting using non-intrusive load monitoring," *Sustainable Energy, Grids and Networks*, vol. 34, 2023, doi: 10.1016/j.segan.2023.101006.

[20] M. D'Incecco, S. Squartini, and M. Zhong, "Transfer Learning

for Non-Intrusive Load Monitoring," *IEEE Trans Smart Grid*, vol. 11, no. 2, 2020, doi: 10.1109/TSG.2019.2938068.

[21] Y. Zhang *et al.*, "FedNILM: Applying Federated Learning to NILM Applications at the Edge," *IEEE Transactions on Green Communications and Networking*, vol. 7, no. 2, 2023, doi: 10.1109/TGCN.2022.3167392.

[22] H. Abbasimehr, M. Shabani, and M. Yousefi, "An optimized model using LSTM network for demand forecasting," *Comput Ind Eng*, vol. 143, 2020, doi: 10.1016/j.cie.2020.106435.

[23] A. Kurani, P. Doshi, A. Vakharia, and M. Shah, "A Comprehensive Comparative Study of Artificial Neural Network (ANN) and Support Vector Machines (SVM) on Stock Forecasting," *Annals of Data Science*, vol. 10, no. 1. 2023. doi: 10.1007/s40745-021-00344-x.

[24] Syaharuddin, Fatmawati, and H. Suprajitno, "Investigations on Impact of Feature Normalization Techniques for Prediction of Hydro-Climatology Data Using Neural Network Backpropagation with Three Layer Hidden," *International Journal of Sustainable Development and Planning*, vol. 17, no. 7, 2022, doi: 10.18280/ijsdp.170707.

[25] C. Zhang, M. Zhong, Z. Wang, N. Goddard, and C. Sutton, "Sequence-to-point learning with neural networks for non-intrusive load monitoring," in *32nd AAAI Conference on Artificial Intelligence, AAAI 2018*, 2018. doi: 10.1609/aaai.v32i1.11873.

[26] S. Guessoum *et al.*, "The Short-Term Prediction of Length of Day Using 1D Convolutional Neural Networks (1D CNN)," *Sensors*, vol. 22, no. 23, 2022, doi: 10.3390/s22239517.

[27] T. Szandała, "Review and comparison of commonly used activation functions for deep neural networks," in *Studies in Computational Intelligence*, vol. 903, 2021. doi: 10.1007/978-981-15-5495-7_11.

[28] D. P. Kingma and J. L. Ba, "Adam: A method for stochastic optimization," in *3rd International Conference on Learning Representations, ICLR 2015 - Conference Track Proceedings*, 2015.

[29] M. P. Moghaddam, A. Abdollahi, and M. Rashidinejad, "Flexible demand response programs modeling in competitive electricity markets," *Appl Energy*, vol. 88, no. 9, 2011, doi: 10.1016/j.apenergy.2011.02.039.

[30] V. Sharifi, A. Abdollahi, and M. Rashidinejad, "Flexibility-based generation maintenance scheduling in presence of uncertain wind power plants forecasted by deep learning considering demand response programs portfolio," *International Journal of Electrical Power and Energy Systems*, vol. 141, 2022, doi: 10.1016/j.ijepes.2022.108225.